Phonon-induced dephasing of localized optical excitations

Phonon-induced dephasing of localized optical excitations

D. Brinkmann, F. Rossi, S. W. Koch, and P. Thomas
Fachbereich Physik und Zentrum für Materialwissenschaften, Philipps-Universität Marburg, Renthof 5, 35032 Marburg, Federal Republic of Germany
(Received 21 December 1995)

The dynamics of strongly localized optical excitations in semiconductors is studied including electron-phonon interaction. The coupled microscopic equations of motion for the interband polarization and the carrier distribution functions contain coherent and incoherent contributions. While the coherent part is solved through direct numerical integration, the incoherent one is treated by means of a generalized Monte Carlo simulation. The approach is illustrated for a simple model system. The temperature and excitation energy dependence of the optical dephasing rate is analyzed and the results are compared to those of alternative approaches. [S0163-1829(96)02328-4]

I. INTRODUCTION

Many semiconductors possess a certain degree of structural disorder. Examples include amorphous and microcrystalline bulk semiconductors, mixed crystalline semiconductors, semiconductor heterostructures, and also polymers. For real systems, the detailed nature of this static disorder is usually not precisely known. However, since disorder has a pronounced influence on the electronic properties of these materials, it is highly desirable to characterize the relevant disorder parameters by applying suitable experimental techniques.

Generally, transport experiments yield only quite global information, and the transport theory of interacting disordered many-particle systems is far from being sufficiently well established. A more sensitive probe for the different interaction processes is the optical polarization. Its dynamics, and, in particular, its phase coherence properties reflect the various interaction processes on an ultrashort time scale. In order to study the combined influence of disorder, many-particle Coulomb interactions and electron-phonon coupling on the optical polarization, one has to solve the semiconductor Bloch equations (SBE)[1] for a disordered semiconductor, where the electron-phonon interaction has to be included explicitly.

It is evident that this program presents a formidable task. As a first step towards such a theory in this paper we concentrate on situations, where the optical excitations are strongly localized due to disorder. The optical spectrum is then dominated by an inhomogeneously broadened line, and experimentally the phase coherence cannot be deduced from the linear spectrum. However, applying the transient four-wave-mixing (FWM) technique, the phase coherence time (or the dephasing rate) can be measured easily. In the time-resolved detection mode of the two-beam degenerate FWM experiment the inhomogeneous line leads to a photon echo. In the time-integrated detection mode (TI), the echo decay for increasing pump-probe pulse separation is monitored.[2,3] The measured echo-decay rate is then identified with the loss of phase coherence. For example, photon echo experiments on CdS_xSe_{1-x} mixed crystals yield extraordinary long phase lifetimes, exceeding 1 ns.[4,5] Furthermore, in this system the dephasing rate has been determined as a function of temperature and excitation energy within the inhomogeneous line.[5]

The description of photon echoes requires the solution of the SBE in third order in the external laser field. For a tight-binding model of a disordered semiconductor, this has been done for arbitrary degree of disorder, however, ignoring the many-particle Coulomb interaction and the phonon coupling.[6] Hence, these studies concentrate only on the influence of purely static disorder on optical phase coherence. Later excitonic excitations in disordered semiconductors with a weak long-range fluctuating disorder potential have been considered,[7] and the relation between phonon-induced transport (hopping) and optical dephasing has been investigated for a model without Coulomb interaction.[8]

Existing theoretical approaches to analyze the temperature dependence of the dephasing rate usually rely on the assumption that the dephasing processes are related either to phonon-assisted transitions of excitations between the localized centers (sites) or to detrapping events above a mobility edge.[9] These approaches are based on the idea that there exists a ''typical'' hop, which is responsible for breaking the phase, although in reality there is an extremely wide distribution of hopping rates in many disordered systems. The ''typical'' hop is then determined by some fitting or optimization procedure.[10,11] In this respect, there is a close resemblance to hopping transport theories. Their prototype, Mott's famous variable range hopping,[12] rests on such an optimization procedure and works perfectly well for some simple situations. In more general cases, i.e., for complicated density-of-states distributions, a numerical analysis of the transport process by, e.g., a Monte Carlo simulation has to be performed.

A more general approach, not relying on ''typical'' hops, does not yet exist. The solution of a rate equation describing the incoherent hopping processes alone is insufficient, since the dynamics of the optical polarization has to be included in the analysis. In order to analyze the decay of coherence in this paper we present an approach which extends working theories for the case of perfect crystalline, i.e., ordered semiconductors.[1] In our numerical evaluation, we follow the procedure[13,14] where the coherent evolution of the polarization is calculated by solving the SBE, while the incoherent

scattering processes are treated within a Boltzmann formalism, which is numerically modeled using a generalized Monte Carlo technique.

While for ordered semiconductors the inclusion of the Coulomb interaction is mandatory, in disordered systems, in particular, if the excitations are sufficiently localized, the neglection of this interaction is not completely unreasonable. Our present approach is, therefore, based on a model excluding the Coulomb interaction, while disorder and phonon coupling are included. We assume that the relevant optical excitations are localized by the disorder potential and that the dephasing interactions are related to phonon-assisted hopping processes. In a real-space formulation, we derive the coherent part of the equation of motion, which resembles the Bloch equations as presented previously,[15] and also the equations governing the incoherent dynamics, which are the well known multiphonon rate equations.[16] This set of equations is then solved simultaneously, making use of a Monte Carlo simulation for the rate equation. The approach is illustrated for a simple model of a disordered semiconductor structure. We calculate the temperature dependence of the dephasing rate and its dependence on excitation energy.

The paper is organized as follows. In Sec. II, we present the model Hamiltonian and evaluate the equations of motion. These equations are applied for a FWM situation in Sec. III. In Sec. IV, we show how the Monte Carlo technique is used to simulate the incoherent dynamics of both the distribution functions and the polarization. Finally, in Sec. V, we introduce a simple model and present the results. Technical details are presented in the Appendixes.

II. BASIC EQUATIONS

A. The model Hamiltonian

Since we want to analyze a strongly disordered material, we choose the site representation in a tight-binding description. We assume diagonal disorder in the following sense: Each site i consists of a two-level absorber with the energies ϵ_i^c and ϵ_i^v for the higher and lower state, respectively. The levels in the upper (lower) band are mutually coupled by J_{ij}^{α} $(\alpha=v,c)$ forming the conduction (valence) band. Thus, the total electron Hamiltonian can be written as

$$H_{\mathrm{el}}=\sum_{i,\alpha}\epsilon_{i,\alpha}\hat{n}_{ii}^{\alpha}+\sum_{i\neq j,\alpha}J_{ij}^{\alpha}\hat{c}_{i,\alpha}^{\dagger}\hat{c}_{j,\alpha}. \tag{1}$$

Neglecting recoil, the electron-phonon coupling A is assumed to be site diagonal:

$$H_{\text{el-ph}}=\sum_{i,q,\alpha}\hat{c}_{i,\alpha}^{\dagger}\hat{c}_{i,\alpha}(A_{i,q}^{\alpha}\hat{a}_q^{\dagger}+A_{i,q}^{\alpha *}\hat{a}_q). \tag{2}$$

The interaction with the light field is treated in the dipole approximation:

$$H_{\mathrm{dipol}}=-\sum_{i=1}^{N}\mu_i E_i(\hat{c}_{i,v}^{\dagger}\hat{c}_{i,c}+\hat{c}_{i,c}^{\dagger}\hat{c}_{i,v}). \tag{3}$$

We define

$$H_0=\sum_{i=1}^{N}\sum_{\alpha=c,v}\epsilon_{i,\alpha}\hat{n}_{ii}^{\alpha}+\sum_q\hbar\omega_q(\hat{a}_q^{\dagger}\hat{a}_q+\tfrac{1}{2}). \tag{4}$$

Note that we do not include Coulomb interaction in our model Hamiltonian. If we are dealing with strongly localized excitations, these interactions can be assumed to be negligible. On the other hand, for some situations, we can interpret our excitations as excitons, so that Coulomb effects are included to some extent.

A canonical transformation eliminates the explicit electron-phonon coupling from the Hamiltonian.[17] Then the transition energies are renormalized and the J overlaps become phonon operators. The Hamiltonian is given by

$$\widetilde{H}=\sum_{i,\alpha}\epsilon_{i,\alpha}\hat{n}_{ii}^{\alpha}+\sum_{i\neq j}\sum_{\alpha=c,v}J_{ij}^{\alpha}e^{S_{ij}^{\alpha}}\hat{c}_{i,\alpha}^{\dagger}\hat{c}_{j,\alpha}+\sum_q\hbar\omega_q \times(\hat{a}_q^{\dagger}\hat{a}_q+\tfrac{1}{2})-\sum_i\mu_i E_i(\hat{c}_{i,v}^{\dagger}\hat{c}_{i,c}+\hat{c}_{i,c}^{\dagger}\hat{c}_{i,v}), \tag{5}$$

where we use the abbreviations:

$$S_{ij}^{\alpha}=\sum_q\frac{1}{\hbar\omega_q}(A_{ij,q}^{\alpha}\hat{a}_q^{\dagger}-A_{ij,q}^{\alpha *}\hat{a}_q),$$

$$A_{ij,q}^{\alpha}=A_{i,q}^{\alpha}-A_{j,q}^{\alpha}. \tag{6}$$

Note that the renormalization of the energies, due to the phonons $[\widetilde{\epsilon}_i=\epsilon_i-\Sigma_q(1/\hbar\omega_q)|A_{i,q}|^2\approx\epsilon_i]$ has been neglected, assuming that disorder dominates the single site energies. The optical transitions become renormalized as well, leading to Urbach tails in the spectrum[18] and an initial fast but incomplete phase relaxation.[8] As we are interested in the phase coherence on time scales comparable to intersite hops, we neglect the renormalization of the optical transitions and concentrate on the long-time behavior.

B. The equations of motion

For simplicity of notation we present, in this subsection, only the derivation of the equations of motion for single-phonon processes. The results for the multiphonon case can be obtained by direct generalization. As far as the density dynamics is concerned, the result is the well known rate equation used in hopping transport theories. The derivation for multiphonon processes is described in the appendix and, to the best of our knowledge, constitutes a new derivation of the multiphonon rate equation of hopping transport theories.[16] The equation of motion for the density operators is given by

$$\frac{\partial}{\partial t}\hat{n}_{ii}^{c}=\frac{i}{\hbar}\sum_{k\neq i}[J_{ki}^{c}\hat{n}_{ki}^{c}(1+S_{ki}^{c})-J_{ik}^{c}\hat{n}_{ik}^{c}(1+S_{ik}^{c})] -\frac{i}{\hbar}\mu_i E_i(\hat{p}_{ii}^{\dagger}-\hat{p}_{ii}), \tag{7}$$

and similar for $\hat{n}_{ii}^{v}$.

Taking the expectation values and factorizing them into a phonon and an electron part shows that the lowest order terms, which contain just a single-phonon operator, always vanish. The first nonvanishing contributions are obtained in

next higher order, which requires that we evaluate the Heisenberg equations for three-point operators. We obtain

$$\frac{\partial}{\partial t}\hat{n}^{\alpha}_{ij}\hat{a}^{\dagger}_{q}=i(\omega^{\alpha}_{ij}+\omega_q)\hat{n}^{\alpha}_{ij}\hat{a}^{\dagger}_{q}+\frac{i}{\hbar}\sum_{k\neq i}J^{\alpha}_{ki}\hat{n}^{\alpha}_{kj}(1+S^{\alpha}_{ki})\hat{a}^{\dagger}_{q}$$
$$-\frac{i}{\hbar}\sum_{k\neq j}J^{\alpha}_{jk}\hat{n}^{\alpha}_{ik}(1+S^{\alpha}_{jk})\hat{a}^{\dagger}_{q}$$
$$-\frac{i}{\hbar}\sum_{kl,\beta}J^{\beta}_{kl}\frac{1}{\hbar\omega_q}A^{\beta *}_{kl,q}\hat{n}^{\alpha}_{ij}\hat{n}^{\beta}_{kl}, \tag{8}$$

and similar for $\hat{n}^{\alpha}_{ij}\hat{a}_q$. For consistency, we neglect here terms describing the simultaneous excitation by phonons and photons, since effects of this nature have already been neglected in the Hamiltonian.

The formal solution of the inhomogeneous differential equations is given by

$$\hat{n}^{\alpha}_{ij}(t)\hat{a}^{\dagger}_{q}(t)=\hat{n}^{\alpha}_{ij}(t_0)\hat{a}^{\dagger}_{q}(t_0)e^{i(\omega^{\alpha}_{ij}+\omega_q)(t-t_0)}$$
$$+\int_{t_0}^{t}dt' e^{i(\omega^{\alpha}_{ij}+\omega_q)(t-t')}\frac{i}{\hbar}$$
$$\times\Bigg(\sum_{k\neq i}J^{\alpha}_{ki}\hat{n}^{\alpha}_{kj}(t')[1+S^{\alpha}_{ki}(t')]\hat{a}^{\dagger}_{q}(t')$$
$$-\sum_{k\neq j}J^{\alpha}_{jk}\hat{n}^{\alpha}_{ik}(t')[1+S^{\alpha}_{jk}(t')]\hat{a}^{\dagger}_{q}(t')$$
$$-\sum_{kl,\beta}J^{\beta}_{kl}\frac{1}{\hbar\omega_q}A^{\beta *}_{kl,q}\hat{n}^{\alpha}_{ij}(t')\hat{n}^{\beta}_{kl}(t')\Bigg).$$

These equations are evaluated in the adiabatic limit using the Markov approximation (see Appendix B). Furthermore, all terms which are nondiagonal in the site indices are neglected [the last terms in Eq. (9) will have site-diagonal contributions after evaluating the expectation values within Hartree-Fock approximation]. In our model, these terms are assumed to be small compared to the site-diagonal densities. In this way only one term from each of the sums ($k\neq j$) contributes. We thus obtain

$$\hat{n}^{\alpha}_{ij}\hat{a}^{\dagger}_{q}(t)=\pi\delta(\omega^{\alpha}_{ij}+\omega_q)\frac{i}{\hbar}$$
$$\times\Bigg(J^{\alpha}_{ji}\hat{n}^{\alpha}_{jj}(1+S^{\alpha}_{ji})\hat{a}^{\dagger}_{q}-J^{\alpha}_{ji}\hat{n}^{\alpha}_{ii}(1+S^{\alpha}_{ji})\hat{a}^{\dagger}_{q}$$
$$-J^{\alpha}_{ji}\frac{1}{\hbar\omega_q}A^{\alpha *}_{ji,q}\hat{n}^{\alpha}_{ij}\hat{n}^{\alpha}_{ji}\Bigg),$$

$$\hat{n}^{\alpha}_{ij}\hat{a}_{q}(t)=\pi\delta(\omega^{\alpha}_{ij}-\omega_q)\frac{i}{\hbar}$$
$$\times\Bigg(J^{\alpha}_{ji}\hat{n}^{\alpha}_{jj}(1+S^{\alpha}_{ji})\hat{a}_{q}-J^{\alpha}_{ji}\hat{n}^{\alpha}_{ii}(1+S^{\alpha}_{ji})\hat{a}_{q}$$
$$-J^{\alpha}_{ji}\frac{1}{\hbar\omega_q}A^{\alpha}_{ji,q}\hat{n}^{\alpha}_{ij}\hat{n}^{\alpha}_{ji}\Bigg). \tag{9}$$

This result is inserted into the equations of motion (7) and then the expectation values are taken, again by decoupling them into an electron and a phonon part. In a next step then the electronic four-point operators are evaluated by making a Hartree-Fock approximation.

The purely coherent part in the resulting equations describe *intraband* coherence, which can be neglected in our model problem, since only hopping processes play a significant role, due to the assumed strong localization. (For a simultaneous treatment of both coherent and incoherent intraband processes see Refs. 19 and 20.)

This way we finally obtain the well known Miller-Abrahams rate equation[21] for the incoherent part of the dynamics:

$$\frac{\partial}{\partial t}n^{e}_{i}|^{\mathrm{inc}}=2\pi\sum_{k\neq i}\sum_{q}|J^{e}_{ki}|^2\frac{|A^{e}_{ki}|^2}{\hbar^2\omega_q^2}$$
$$\times\{n^{e}_{k}[1-n^{e}_{i}][\delta(\omega^{e}_{ki}+\omega_q)N_q$$
$$+\delta(\omega^{e}_{ki}-\omega_q)(N_q+1)]$$
$$-n^{e}_{i}[1-n^{e}_{k}][\delta(\omega^{e}_{ki}+\omega_q)(N_q+1)$$
$$+\delta(\omega^{e}_{ki}-\omega_q)N_q]\}. \tag{10}$$

(The second index of the densities is suppressed, since only diagonal terms appear in these equations.) Note that we now use an electron-hole representation, i.e., $n^{e}_{i}=n^{c}_{i}$ and $n^{h}_{i}=1-n^{v}_{i}$. The corresponding equation for the holes is obtained by replacing n^{e}_{i} with $1-n^{h}_{i}$. The full equations of motion for the densities are given by

$$\frac{\partial}{\partial t}n^{e}_{i}=\frac{i}{\hbar}\mu E(p^{*}_{i}-p_i)+\frac{\partial}{\partial t}n^{e}_{i}|^{\mathrm{inc}},$$

$$\frac{\partial}{\partial t}n^{h}_{i}=\frac{i}{\hbar}\mu E(p^{*}_{i}-p_i)+\frac{\partial}{\partial t}n^{h}_{i}|^{\mathrm{inc}}. \tag{11}$$

A similar procedure as described above can be performed for the polarization. Here we give only the final result:

$$\frac{\partial}{\partial t}p_i|^{\mathrm{inc}}=\frac{1}{\hbar^2}\sum_{k\neq i}\sum_{q}\Bigg\{-\frac{|J^{h}_{ik}|^2}{\omega_q^2}\{(N_q+1-n^{h}_{k})|A^{h}_{ik}|^2\mathcal{D}(\omega^{h}_{ik}$$
$$+\omega_q)+(N_q+n^{h}_{k})|A^{h}_{ik}|^2\mathcal{D}(\omega^{h}_{ik}-\omega_q)\}p_i$$
$$-\frac{|J^{e}_{ik}|^2}{\omega_q^2}\{(N_q+1-n^{e}_{k})|A^{e}_{ik}|^2\mathcal{D}(\omega^{e}_{ik}-\omega_q)$$
$$+(N_q+n^{e}_{k})|A^{e}_{ik}|^2\mathcal{D}(\omega^{e}_{ik}+\omega_q)\}p_i$$
$$+\frac{J^{e}_{ki}J^{h}_{ik}}{\omega_q^2}\{(N_q+1-n^{h}_{i})A^{e}_{ik}A^{h *}_{ik}\mathcal{D}(\omega^{h}_{ik}-\omega_q)$$
$$+(N_q+n^{h}_{i})A^{h}_{ik}A^{e *}_{ik}\mathcal{D}(\omega^{h}_{ik}+\omega_q)\}p_k$$
$$+\frac{J^{e}_{ki}J^{h}_{ik}}{\omega_q^2}\{(N_q+1-n^{e}_{i})A^{h}_{ik}A^{e *}_{ik}\mathcal{D}(\omega^{e}_{ik}+\omega_q)$$
$$+(N_q+n^{e}_{i})A^{e}_{ik}A^{h *}_{ik}\mathcal{D}(\omega^{e}_{ik}-\omega_q)\}p_k\Bigg\}. \tag{12}$$

The Dirac-distribution $\mathcal{D}(x)=[1/(ix+\eta)]=-i(\mathcal{P}/x)+\pi\delta(x)$ has been introduced since, in contrast to the densities, the polarization is not a real quantity.

The full equation of motion for the polarization is then given by

$$\frac{\partial}{\partial t}p_i=\omega_i p_i+\mu E(n_i^e+n_i^h-1)+\frac{\partial}{\partial t}p_i|^{\mathrm{inc}}. \tag{13}$$

The coupled equations (10)–(13) are the full set of equations describing the dynamics of the densities and polarization in our system with single-phonon processes being the only incoherent scattering mechanisms. For multiphonon processes, one has to use the equations derived in Appendix A.

III. FOUR-WAVE MIXING

Here, we restrict ourselves to the experimental situation of two-pulse degenerate four-wave mixing, where two pulses with wave vectors $\vec{k}_1$ and $\vec{k}_2$ hit the sample at time 0 and τ, respectively, both having the same frequency ω_L. Hence, the optical field is given by

$$E(t)=E_1^0(t)(e^{i(\vec{k}_1\cdot\vec{r}-\omega_L t)}+e^{-i(\vec{k}_1\cdot\vec{r}-\omega_L t)})+E_2^0(t)\times(e^{i(\vec{k}_2\cdot\vec{r}-\omega_L t)}+e^{-i(\vec{k}_2\cdot\vec{r}-\omega_L t)}). \tag{14}$$

The envelope functions E_i^0 of the pulses are chosen to be Gaussian in the numeric calculations, which is close to reality.

In order to derive the equations of motion for the four-wave-mixing geometry, we use a spatial Fourier series expansion.[22] We are interested in the equation of motion for the polarization function in the direction $2\vec{k}_2-\vec{k}_1$. Furthermore, we restrict ourselves to the contributions obtained in the lowest order of the applied field. In this way, we only need to consider the following quantities:

$$\frac{\partial}{\partial t}p_i^{(1|0)}=-\frac{i}{\hbar}[\omega_i p_i^{(1|0)}-\mu E_1^0(t)e^{i(\vec{k}_1\cdot\vec{r}-\omega_L t)}]-\frac{\partial}{\partial t}p_i^{(1|0)}|^{\mathrm{inc}}, \tag{15}$$

$$\frac{\partial}{\partial t}p_i^{(0|1)}=-\frac{i}{\hbar}[\omega_i p_i^{(0|1)}-\mu E_2^0(t)e^{i(\vec{k}_2\cdot\vec{r}-\omega_L t)}]-\frac{\partial}{\partial t}p_i^{(0|1)}|^{\mathrm{inc}}, \tag{16}$$

$$\frac{\partial}{\partial t}n_i^{e(-1|1)}=\frac{i}{\hbar}\mu[E_2^0(t)e^{i(\vec{k}_2\cdot\vec{r}-\omega_L t)}p_i^{(1|0)*}-E_1^0(t)e^{i(\vec{k}_1\cdot\vec{r}-\omega_L t)}p_i^{(0|1)}]-\frac{\partial}{\partial t}n_i^{e(-1|1)}|^{\mathrm{inc}}, \tag{17}$$

$$\frac{\partial}{\partial t}n_i^{h(-1|1)}=\frac{i}{\hbar}\mu[E_2^0(t)e^{i(\vec{k}_2\cdot\vec{r}-\omega_L t)}p_i^{(1|0)*}-E_1^0(t)e^{i(\vec{k}_1\cdot\vec{r}-\omega_L t)}p_i^{(0|1)}]-\frac{\partial}{\partial t}n_i^{h(-1|1)}|^{\mathrm{inc}}, \tag{18}$$

$$\frac{\partial}{\partial t}p_i^{(-1|2)}=-\frac{i}{\hbar}[\omega_i p_i^{(-1|2)}+\mu E_2^0(t)e^{i(\vec{k}_2\cdot\vec{r}-\omega_L t)}(n_i^{e(-1|1)}+n_i^{h(-1|1)})]-\frac{\partial}{\partial t}p_i^{(-1|2)}|^{\mathrm{inc}}. \tag{19}$$

The superscript $(n|m)$ indicates the direction $\vec{k}=n\vec{k}_1+m\vec{k}_2$. For the incoherent part, we obtain

$$\frac{\partial}{\partial t}p_i|^{\mathrm{inc}}=\pi\sum_{k\neq i}\left\{-\frac{|A_{ik}^e|^2}{(\hbar\omega_{ik}^e)^2}\left|J_{ik}^e\right|^2\mathcal{N}_{ki}^e p_i+\frac{A_{ik}^e A_{ik}^h}{(\hbar\omega_{ik}^e)^2}J_{ki}^e J_{ik}^h\mathcal{N}_{ik}^e p_k-\frac{|A_{ik}^h|^2}{(\hbar\omega_{ik}^h)^2}\left|J_{ik}^h\right|^2\mathcal{N}_{ik}^h p_i+\frac{A_{ik}^h A_{ik}^e}{(\hbar\omega_{ik}^h)^2}J_{ki}^e J_{ik}^h\mathcal{N}_{ki}^h p_k\right\}, \tag{20}$$

$$\frac{\partial}{\partial t}n_i^{e(-1|1)}|^{\mathrm{inc}}=2\pi\sum_{k\neq i}\frac{|A_{ki}^e|^2}{(\hbar\omega_{ik}^e)^2}|J_{ki}^e|^2\{\mathcal{N}_{ki}^e n_k^{e(-1|1)}-\mathcal{N}_{ik}^e n_i^{e(-1|1)}\}, \tag{21}$$

$$\frac{\partial}{\partial t}n_i^{h(-1|1)}|^{\mathrm{inc}}=2\pi\sum_{k\neq i}\frac{|A_{ki}^h|^2}{(\hbar\omega_{ik}^h)^2}|J_{ki}^h|^2\{\mathcal{N}_{ki}^h n_k^{h(-1|1)}-\mathcal{N}_{ik}^h n_i^{h(-1|1)}\}. \tag{22}$$

Note that Eq. (20) is valid both for the first order ($p_i^{(1|0)}$ and $p_i^{(0|1)}$) and for the third order signal ($p_i^{(-1|2)}$). We have approximated the $\mathcal{D}$ distributions by their real parts, $[\mathcal{D}(x)\approx\pi\delta(x)]$. As the wave functions of our model are real quantities, we thus only neglect a slight rotation of the quantities, which means a small shift of the resonance energies. This approximation allows us to evaluate the sums over q using the δ function. Furthermore, we introduced the following abbreviation for the phonon occupation number:

$$\mathcal{N}_{ik}=\begin{cases}N_{ik}+1 & : \quad E_i>E_k\\ N_{ki} & : \quad E_i<E_k,\end{cases} \tag{23}$$

$$N_{ik}=\left[\exp\left(\frac{\hbar(\omega_i-\omega_k)}{kT}\right)-1\right]^{-1}. \tag{24}$$

The equations (15)–(22) form a closed set, which we evaluate in the following.

IV. THE MONTE CARLO APPROACH

Our task is to solve Eqs. (15)–(22). Since this is a coupled system of equations, we introduce a time discretization in terms of a fixed time step δt. Over such a time step, the coherent dynamics is decoupled from the incoherent one. The coherent part of our equations is solved by means of a direct numerical integration from t to $t+\delta t$ evaluating all nonlinear quantities at the beginning of the time step. On the contrary, the incoherent part of our SBE is ''sampled'' by means of a generalized Monte Carlo (MC) simulation.

Now we give a short introduction to the Monte Carlo

simulations used in the framework of hopping transport theories. Unfortunately, we are forced to modify this MC technique, since our kinetic variables are, in general, complex quantities, e.g., the optical polarization. For perfectly ordered semiconductors, an analogous approach has been developed previously by Rossi *et al.*[13,14]

The conventional Monte Carlo method used for the study of transport phenomena can be regarded from a more general point of view as a stochastic approach for the solution of the Boltzmann transport equation:

$$\frac{\partial}{\partial t} f_i|^{\mathrm{inc}} = \sum_k \left[\Gamma_{ki} f_k - \Gamma_{ik} f_i\right]. \tag{25}$$

At first glance, one recognizes the out-scattering proportional to f_i and the in-scattering proportional to f_k with Γ being the corresponding scattering rates. Introducing the Boltzmann propagator $G_{k,i}(t,t_0)$, which describes the time evolution during the interval $[t,t_0]$, the equation can be rewritten:

$$f_i(t) = \sum_k G_{k,i}(t,t_0) N_k(t_0) w_k . \tag{26}$$

With N_k we denote the number of particles starting at site k, which is given by

$$N_k(t_0) = \frac{f_k(t_0)}{\Sigma_i f_i(t_0)} N_S . \tag{27}$$

Here, N_S is the number of simulated particles, while w_k is the relative weight of the site k being equal for all sites in this kind of simulation:

$$w = w_k = \frac{\Sigma_i f_i(t_0)}{N_S}. \tag{28}$$

The Monte Carlo evaluation of the sum Eq. (26) is done by generating a given number N_S of simulative particles and by assigning to each of them an initial site. During the time interval $[t,t_0]$ scattering due to the corresponding rates Γ takes place. A scattering process means that the particle is taken away from its site and put into the destination site. In this way, we get the densities $f_k(t)$ as functions of the initial distributions $f_k(t_0)$ and of the scattering rates $\Gamma_{i,j}$.

We want to stress that the situation in our case is different: Here the coherence of the system has not yet been damped out, i.e., the interplay between the coherent and incoherent dynamics may be important. Consequently, we have to include the polarization dynamics, in particular, the incoherent evolution of the polarization. In addition, the intraband quantities that we are dealing with are not necessarily real quantities in a FWM experiment. Thus, we have to extend the method given above in order to describe the scattering of complex quantities within the Monte Carlo approach.

This is done as follows: We use the same description as above with two differences. (i) The initial number of particles at site k is given according to the modulus of the now complex quantity f_k:

$$N_k(t_0) = \frac{|f_k(t_0)|}{\Sigma_j |f_j(t_0)|} N_S . \tag{29}$$

(ii) The relative weight of a particle starting at site k includes the phase of the site:

$$w_k = \frac{\Sigma_j |f_j(t_0)|}{N_S} \frac{f_k(t_0)}{|f_k(t_0)|} = \frac{\Sigma_j |f_j(t_0)|}{N_S} \exp(i\phi_k). \tag{30}$$

A detailed discussion of a MC simulation with complex quantities is given by Haas, Rossi, and Kuhn.[23] As mentioned above, this kind of MC simulation has to be done for the polarizations, as well as for the distribution functions. Finally, we want to stress that the MC solution of the polarization dynamics has to be done extremely carefully as the rate for the in and out scattering can be very different, so that numerical instabilities are likely to occur.

V. THE MODEL SYSTEM

At this point, we have now derived a closed set of equations describing the phonon-induced dephasing of strongly localized optical excitations. These equations are valid for a relatively large class of three-dimensional systems. In the remainder of this paper, we will now illustrate our approach on the example of a simple model system. For this system, we analyze the time evolution of the intensity of the FWM signal, i.e., the dephasing rate, and we study the temperature dependence of this rate. Next, we then assume excitation by spectrally narrow laser pulses focused to different spectral regions of the inhomogeneous optical line, in order to study the dependence of the dephasing rate on excitation energy. Finally, we compare the results with approaches where the dephasing rate has been identified with a ''typical'' hopping rate.

As a model system, we take a multiple quantum-well system. The width of each quantum well is chosen randomly, such that the density of states for the lowest confinement energies has a Gaussian shape. We only consider the energetically lowest confined states. In this way, each quantum well is modeled as a two-level absorber where, however, phonon-assisted tunneling between the wells is included. Furthermore, our model also describes situations where excitons are strongly localized in quantum wells and are able to perform phonon-assisted tunneling from well to well. In this sense, the linear part of the attractive interband Coulomb interaction is included.

A. The numerical approach

We use the well known particle-in-a-box model to evaluate the lowest confined states for electrons and holes in each quantum well. The effective masses are taken as $m_{\mathrm{eff},e} = 0.063 m_0$ and $m_{\mathrm{eff},h} = 0.450 m_0$. Due to the different effective masses and the different confinement potentials, we obtain a Gaussian density of states with the width of 30 meV for electrons and 3 meV for holes. The transfer matrix elements J_{ij}^{α} between wells i and j depend exponentially on the distance r_{ij}:

$$J_{ij} = \langle \psi_i | H | \psi_j \rangle \approx c \exp(-\min\{\kappa_1, \kappa_2\} r_{ij}). \tag{31}$$

The decay parameters κ_i are given by

$$\kappa_i^e = \sqrt{\frac{2 m_{\mathrm{eff},e}}{\hbar^2} (E_{\mathrm{gap}} - E_i^e)} \tag{32}$$

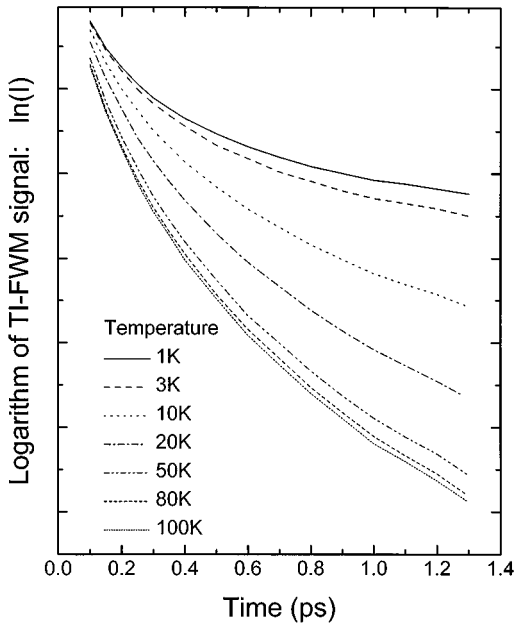

FIG. 1. Time-integrated FWM signal as a function of delay time for various temperatures.

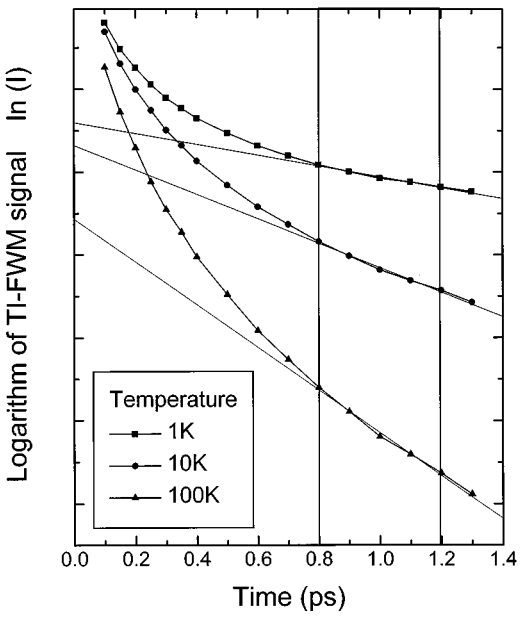

FIG. 2. Definition of the dephasing rate for a limited time interval.

for electrons and

$$\kappa_i^h = \sqrt{\frac{2m_{\text{eff},h}}{\hbar^2}(E_i^h)}. \tag{33}$$

for holes. The electron-phonon coupling constant $A^{\alpha}_{ik,q}$ is modeled by introducing the so-called attempt-to-escape frequency ν_0, which we take as a phenomenological constant:

$$\nu_0 = 2\pi \frac{|A^{\alpha}_{ik,q}|^2}{\hbar^2 \omega_q^2}. \tag{34}$$

We use the value $\nu_0 = 1\times 10^5$ ps^{-1}. The Rabi frequency is chosen to be $\Omega = (\mu E_0/\hbar) = 1$ ps^{-1}. We do not limit the spectrum of the phonons at their Debye energy. In this way, we roughly account for multiphonon processes.

B. Results

For illustration, we first assume extremely short laser pulses modeled as δ pulses. These pulses excite the whole density-of-states (DOS) profile, and photon echoes appear in the time-resolved signal. The polarization at each site decays with its specific rate, but the total polarization, which is a sum of all the polarizations at the various sites, does not decay exponentially. Figure 1 shows the natural logarithm of the computed intensity of the time-integrated FWM signal versus the delay τ for different temperatures. Although the decay is not exponential, it is useful to describe the dephasing process with only a few parameters. Many authors introduce a finite number of decay parameters in order to fit a nonexponential decay. In this way one gets a few phenomenological dephasing rates, each of them being valid only in a specific time interval. We use this method to extract a dephasing rate, which is valid in the time interval 0.8 ps – 1.2 ps. In Fig. 2, we demonstrate for three temperatures how this dephasing rate is obtained. We plot the resulting T_2 time, i.e., the inverse dephasing rate, as a function of the temperature in Fig. 3. It is evident that T_2 decreases strongly with increasing temperature. The physical reason for this behavior is the increasing likelihood of phonon absorption at higher temperatures. For low temperatures only phonon emission processes contribute which are temperature insensitive.

Another method to characterize the dephasing process is to fit the decaying signal with a stretched exponential:

$$I(\tau) = I_0 \exp\left(-\left[\frac{4\tau}{T_2}\right]^{\beta}\right). \tag{35}$$

If the dephasing exhibits this so-called Kohlrausch-Williams-Watt[24] behavior, we get a straight line with slope β and an intersection point $\beta \ln(T_2/4)$ when plot-

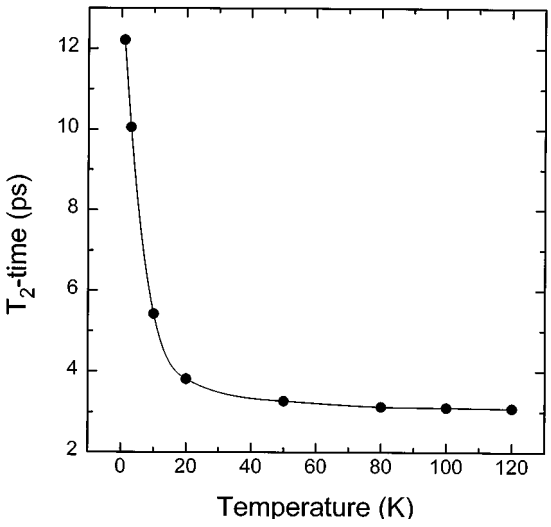

FIG. 3. Dephasing times T_2, determined according to Fig. 2, as a function of temperature.

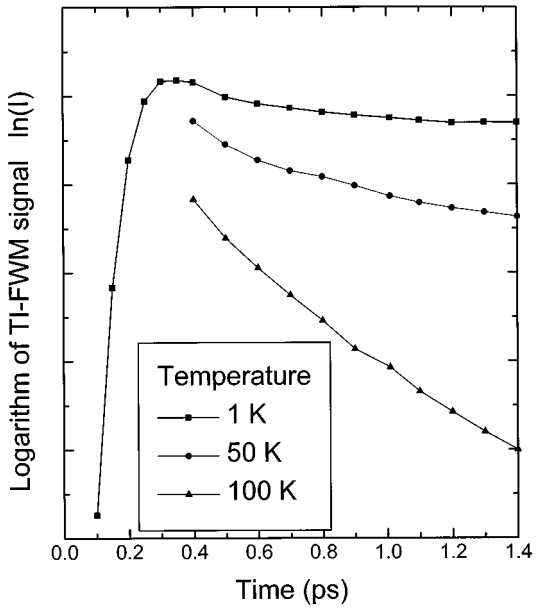

FIG. 4. Time-integrated FWM signal as a function of delay time for excitation in the low-energy region of the density-of-states profile, showing strong temperature dependence.

ting $\ln(-\ln(I/I_0))$ versus $\ln(\tau)$. However, this description also turns out to be only very roughly valid for the model considered here.

In order to study the dependence of dephasing on excitation energy, we assume laser pulses with a duration of 100 fs, which excite only a small part of the DOS. If we excite at 1.27 eV, i.e., at the high-energy side of the DOS, almost all neighbors of excited sites have a lower energy. Thus downward hops dominate the dephasing and no temperature dependence of the dephasing can be seen.

On the other hand, there is a strong temperature dependence if the excition occurs in the low-energy part of the DOS (1.15 eV) (cf. Fig. 4). Again, we can estimate a dephasing rate Γ for the time interval [0.8 ps–1.2 ps]. The temperature dependence of the rates is shown in Fig. 5. Although the

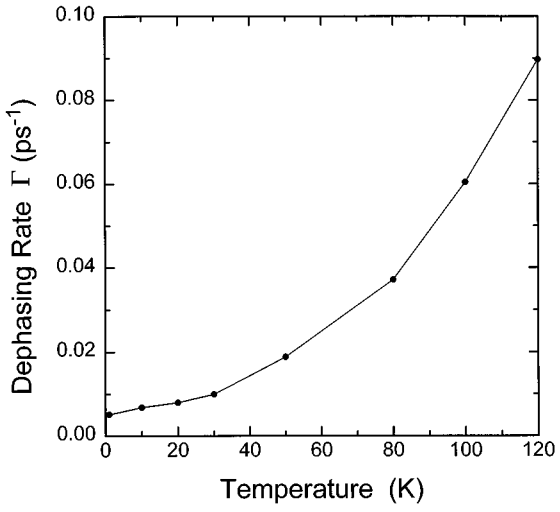

FIG. 5. Temperature dependence of the dephasing rate determined from Fig. 4, according to the procedure illustrated in Fig. 2.

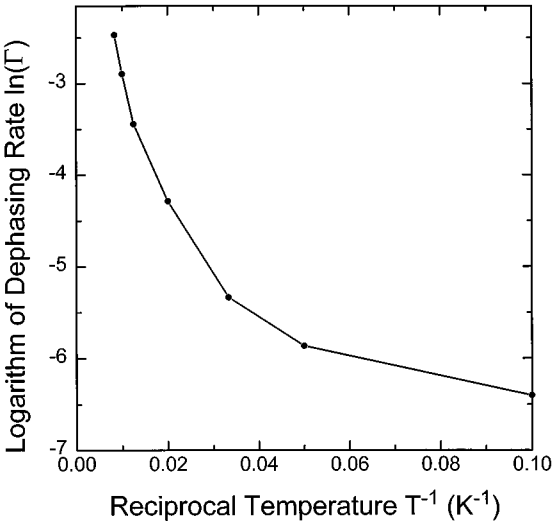

FIG. 6. Same data as in Fig. 5 plotted against T^{-1} showing the strong deviation from an activated behavior.

rate increases with rising temperature, there is no activated behavior, as can be seen in Fig. 6. This observation can be interpreted on the basis of the so-called transport energy,[11,25] which separates those regions in the DOS, where hopping is predominantly activated upwards, from regions where hops occur mainly downwards. This transport energy itself depends on temperature, thus producing the nonactivated behavior.

The situation is completely different for high-energy excitation, as shown in Fig. 7. Here we investigate two different situations, as indicated by the insets to Fig. 7. The temperature was chosen to be 1 K in order to have only downward hops. The dots in Fig. 7 show the computed TI-FWM signal and the solid line is a linear regression showing that the dephasing is now exponential. This is easily under-

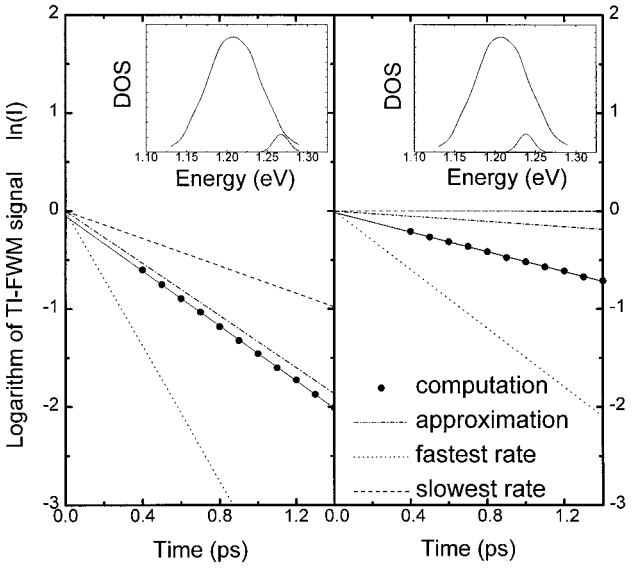

FIG. 7. Time-integrated FWM signal as a function of delay time for two different excitation energies in the high-energy region of the density-of-states profile (dots). The ''typical hop'' approximation is given by the dashed-dotted line.

stood if we note that for excitation high in the DOS nearly all hops are terminated at a site with lower energy, and there is no large dispersion of hopping rates. To be more specific, we note that the electronlike out scattering is the main contribution for the parameters that we used for Fig. 7, so that the other three contributions (electronlike in-scattering, holelike in-scattering, and out-scattering) can be neglected. We can then make a simple approximation of the dephasing rate (see Ref. 25):

$$\nu_{\downarrow}(E_L)=2\frac{\nu_0}{2}\exp\left(-\frac{2R(E_L)}{\alpha}\right), \tag{36}$$

where we introduce a typical downward hop to a site at the mean distance $R(E_L)$. This distance can be obtained by integrating the one-dimensinal DOS $g(E)$ up to the laser energy:

$$R(E_L)=\left[\int_{-\infty}^{E_L} g(x)dx\right]^{-1}. \tag{37}$$

The factor 2 in Eq. (36) reflects the fact that for weak disorder, both the left- and right-hand neighbors have to be taken into account. The localization length α is approximated by that of a site with the energy E_L. This approximation is plotted in Fig. 7 as dash-dotted lines. For comparision, we also plotted the fastest and the slowest rates corresponding to the smallest and largest distances to the next neighbors (remember that only the spatial disorder influences these rates). Clearly the approximation is nearly perfect for excitation at the top of the DOS (left graph), while it deviates strongly for lower excitation energy (right graph). The description of dephasing using just the ''typical'' hop can, therefore, be highly misleading in general.

VI. CONCLUSIONS

We have developed a set of equations describing the dynamics of localized optical excitations including electron-phonon interaction. To study the dephasing of these excitations, we applied our method to the FWM geometry. We have shown how the Monte Carlo technique can be used in order to calculate the incoherent part of the equations of motion. As an illustration, we considered a simple disordered one-dimensional model system. The temperature and excitation dependence of the dephasing rate has been studied and limitations of previous approximate approaches have been demonstrated.

ACKNOWLEDGMENTS

This work has been supported by the Deutsche Forschungsgesellschaft through the Sonderforschungsbereich 383.

APPENDIX A: MULTIPHONON RATE EQUATION

We give a derivation of the multiphonon rate equation by applying the procedure presented in the body of this paper for single-phonon processes. The Hamiltonian containing multiphonon processes reads

$$\tilde{H}=\sum_{i,\alpha}\epsilon_{i,\alpha}\hat{n}^{\alpha}_{ii}+\sum_{i\neq j}\sum_{\alpha=c,v}J^{\alpha}_{ij}e^{S^{\alpha}_{ij}}\hat{c}^{\dagger}_{i,\alpha}\hat{c}_{j,\alpha}+\sum_{q}\hbar\omega(\hat{a}^{\dagger}_{q}\hat{a}_{q}+\tfrac{1}{2})$$
$$-\sum_{i}\mu_i E_i(\hat{c}^{\dagger}_{i,v}\hat{c}_{i,c}+\hat{c}^{\dagger}_{i,c}\hat{c}_{i,v}). \tag{A1}$$

The equations of motion for $\hat{n}^{\alpha}_{ij}$ is (upper sign for $\hat{n}^{v}_{ij}$ and lower for $\hat{n}^{c}_{ij}$)

$$\frac{\partial}{\partial t}n_{ij}=i\omega_{ij}n_{ij}+\frac{i}{\hbar}\sum_{k\neq i}J_{ki}n_{kj}e^{S_{ki}}-\frac{i}{\hbar}\sum_{k\neq j}J_{jk}n_{ik}e^{S_{jk}}$$
$$\pm\frac{i}{\hbar}\mu E(\hat{p}^{\dagger}_{ij}-\hat{p}_{ij}). \tag{A2}$$

For the rest of this appendix, we suppress the index α, since only one band is involved. Because of terms like $n_{ik}e^{S_{jk}}$ and $n_{kj}e^{S_{ki}}$ this set of equations is not closed. A procedure analogous to that used in Sec. II B consists of evaluting the equations of motion for these quantities. However, the resulting equations turn out not to be closed either. After applying the Markov and adiabatic limit, the resulting differential equations can unfortunately not be solved without neglecting important processes.

Thus, a different approach is needed. The idea is to expand the exponential containing the phonon operators and solve the equation of motion for each of these coefficients separately. In this way, no problems arise when solving the differential equations. The resulting equations are then summed up and the well known multiphonon rate equation is obtained. We expand the exponential,

$$e^{S_{ij}}=\sum_{\nu=0}^{\infty}\frac{1}{\nu!}(S_{ij})^{\nu}=\sum_{\nu=0}^{\infty}\frac{1}{\nu!}\left(\sum_{q}\frac{1}{\hbar\omega_q}(A_{ij,q}\hat{a}^{\dagger}_{q}-A^{*}_{ij,q}\hat{a}_{q})\right)^{\nu}$$
$$=\sum_{\nu=0}^{\infty}\frac{1}{\nu!}\sum_{q_1\cdots q_\nu}\frac{1}{\hbar\omega_{q_1}\cdots\hbar\omega_{q_\nu}}$$
$$\times\sum_{\text{binom}}(A^{\bigcirc}_{ij,q_1}\cdots A^{\bigcirc}_{ij,q_\nu})W^{\nu}. \tag{A3}$$

The *binom* sum is a sum over all the 2^{ν} binomial terms of the ν-fold product $(S_{ij})^{\nu}$. W^{ν} is an abbreviation for $\hat{a}^{\bigcirc}_{q_1}\cdots\hat{a}^{\bigcirc}_{q_\nu}$, where $\hat{a}^{\bigcirc}_{q_n}$ can be either a creation or a destruction operator. Note that the operator $n_{ij}W^{\nu}$ contains ν phonon operators, each of which can be either a creation or a destruction operator. Nevertheless, it is possible to evaluate the Heisenberg equation for this very general operator. By neglecting, as mentioned above, all nondiagonal terms and the interaction with the light field, we obtain

$$\frac{\partial}{\partial t}n_{ij}W^{\nu}=i\omega_{ij}n_{ij}W^{\nu}+i\sum_{\lambda=1}^{\nu}\pm\omega_{q_\lambda}n_{ij}(W^{\nu}+W^{\tau<\nu})$$
$$+\frac{i}{\hbar}J_{ji}e^{S_{ji}}(n_{jj}-n_{ii})W^{\nu}$$
$$+\frac{i}{\hbar}J_{ji}n_{ij}n_{ji}[e^{S_{ji}},W^{\nu}]. \tag{A4}$$

In the sum, the plus sign has to be taken if the λth operator of W^{ν} is a creation operator, and the minus is valid if it is a destruction operator.

Here we introduced the operator $W^{\tau<\nu}$: The commutation of W^{ν} with the phonon part of the Hamiltonian reproduces W^{ν} and an additional term (which we denote with $W^{\tau<\nu}$) if at least two-phonon operators have the same q value. However, this additional term has less phonon operators than W^{ν} (therefore the name $W^{\tau<\nu}$). Furthermore, it is an inhomogeneity in the differential equation Eq. (A4) and, in addition, it is nondiagonal with respect to the electronic indices. Hence, it will be neglected like all other quantities that are nondiagonal in the electronic indices. Solving the equation Eq. (A4) and performing the Markov and adiabatic limit yields

$$\begin{aligned} n_{ij}(t)W^{\nu}(t) = & \frac{i}{\hbar}J_{ji}[n_{jj}(t)-n_{ii}(t)] \\ & \times \int_0^{\infty} dt' e^{i(\omega_{ij}+\Sigma\pm\omega_{q_\lambda})t'} e^{S_{ji}(t')} W^{\nu}(t') \\ & + \frac{i}{\hbar}J_{ji}(n_{ji}(t)n_{ij}(t)) \int_0^{\infty} dt' e^{i(\omega_{ij}+\Sigma\pm\omega_{q_\lambda})t'} \\ & \times [e^{S_{ji}(t')}, W^{\nu}(t')]. \end{aligned} \tag{A5}$$

Summing up all the solutions according to Eq. (A3) gives the time evolution of $n_{ij}(t)e^{S_{ij}}(t)$:

$$\begin{aligned} n_{ij}(t)e^{S_{ij}}(t) = & \frac{i}{\hbar}J_{ji}[n_{jj}(t)-n_{ii}(t)] \int_0^{\infty} dt' e^{i\omega_{ij}t'} e^{S_{ji}(t')} e^{S_{ij}(0)} \\ & + \frac{i}{\hbar}J_{ji}(n_{ji}(t)n_{ij}(t)) \int_0^{\infty} dt' e^{i\omega_{ij}t'} \\ & \times [e^{S_{ji}(t')}, e^{S_{ij}(0)}]. \end{aligned} \tag{A6}$$

Thus, the incoherent part of the equation of motion for n_{ii} is given by

$$\begin{aligned} \frac{\partial}{\partial t}n_{ii}\bigg|^{\text{incoh}} = & \frac{i}{\hbar}\sum_{k\neq i} J_{ki}(n_{ki}e^{S_{ki}} - n_{ik}e^{S_{ik}}) \\ = & -\sum_{k\neq i}\frac{|J_{ik}|^2}{\hbar^2}\Bigg[[n_{ii}(t)-n_{kk}(t)]\int_{-\infty}^{0} dt' e^{-i\omega_{ki}t'} \\ & \times e^{S_{ik}(t')}e^{S_{ki}(0)} \\ & + n_{ki}(t)n_{ik}(t)\int_{-\infty}^{0} dt' e^{-i\omega_{ki}t'}[e^{S_{ik}(t')}, e^{S_{ki}(0)}] \\ & - [n_{kk}(t)-n_{ii}(t)]\int_{-\infty}^{0} dt' e^{-i\omega_{ik}t'} e^{S_{ki}(t')} e^{S_{ik}(0)} \\ & - n_{ik}(t)n_{ki}(t)\int_{-\infty}^{0} dt' e^{-i\omega_{ik}t'}[e^{S_{ki}(t')}, e^{S_{ik}(0)}]\Bigg]. \end{aligned} \tag{A7}$$

The last step is now to take the expectations values. After rearranging the resulting terms, the final result is

$$\begin{aligned} \frac{\partial}{\partial t}n_{ii}\bigg|^{\text{incoh}} = & \sum_{k\neq i}\frac{|J_{ik}|^2}{\hbar^2}\Bigg[n_{kk}(1-n_{ii})\int_{-\infty}^{\infty} dt' e^{-i\omega_{ki}t'} Q_{ik} \\ & - n_{ii}(1-n_{kk})\int_{-\infty}^{\infty} dt' e^{-i\omega_{ik}t'} Q_{ki}\Bigg]. \end{aligned} \tag{A8}$$

The expectation values for the phonon operators can be found in the literature:[17]

$$\begin{aligned} Q_{ik}(t) = & \langle e^{S_{ik}(0)} e^{S_{ki}(-t')}\rangle_{\text{ph}} \\ = & \exp\Bigg[-\sum_q \left|\frac{A_{ik,q}}{\hbar\omega_q}\right|^2 \{(N_q+1)(1-e^{-i\omega_q t}) \\ & + N_q(1-e^{i\omega_q t})\}\Bigg]. \end{aligned} \tag{A9}$$

Equation (A8) is the well known multiphonon rate equation.[16] Usually, it is written in the form

$$\begin{aligned} \frac{\partial}{\partial t}n_{ii}\bigg|^{\text{incoh}} = & \sum_{k\neq i}\frac{|J_{ik}|^2}{\hbar^2}\Bigg[n_{kk}(1-n_{ii})e^{-2S}\int_{-\infty}^{\infty} dt' e^{-i\omega_{ki}t'} e^{\phi(t')} \\ & - n_{ii}(1-n_{kk})e^{-2S}\int_{-\infty}^{\infty} dt' e^{-i\omega_{ik}t'} e^{\phi(t')}\Bigg], \end{aligned} \tag{A10}$$

with the definitions

$$\begin{aligned} 2S = & \sum_q \left|\frac{A_{ik,q}}{\hbar\omega_q}\right|^2 \{(2N_q+1)\}, \\ \phi(t') = & \sum_q \left|\frac{A_{ik,q}}{\hbar\omega_q}\right|^2 \{(N_q+1)(e^{-i\omega_q t}) + N_q(e^{i\omega_q t})\}. \end{aligned} \tag{A11}$$

APPENDIX B: MARKOV LIMIT AND ADIABATIC LIMIT

When solving the equations of motion for the dynamical variables, one often obtains differential equations of the form

$$\frac{\partial}{\partial t}x(t) = i\omega x(t) + y(t). \tag{B1}$$

The solution of this differential equation is

$$x(t) = x(t_0)e^{i\omega(t-t_0)} + \int_{t_0}^{t} e^{i\omega(t-t')} y(t') dt'. \tag{B2}$$

This exact solution can be simplified by introducing a number of approximations.

The first one is the Markov limit. Assuming that the temporal variation of the function $y(t)$ is very slow compared to the exponential, it can be treated as a constant within the interval $[t_0, t]$ and thus be taken out of the integral,

$$x(t) \approx x(t_0)e^{i\omega(t-t_0)} + y(t)\int_{t_0}^{t} e^{i\omega(t-t')} dt'. \tag{B3}$$

Then the adiabatic limit is performed. The frequency ω is substituted by $\omega + i\eta$. Furthermore, the lower limit t_0 goes to $-\infty$. Thus, performing the adiabatic limit means that the

influence of any initial contribution has died out:

$$x(t) \approx x(-\infty) e^{i(\omega + i\eta)\infty} + y(t) \int_{-\infty}^{t} e^{i(\omega + i\eta)(t-t')} dt'$$

$$\approx y(t) \int_{-\infty}^{t} e^{i(\omega + i\eta)(t-t')} dt'.$$

Integrating and using the Dirac identity yields

$$x(t) = \left(-i \frac{\mathcal{P}}{\omega} + \pi \delta(\omega) \right) y(t). \tag{B4}$$

If x is a real quantity, this can be simplified further:

$$x(t) = \pi \delta(\omega) y(t). \tag{B5}$$

[1] For a textbook discussion and further references, see H. Haug and S.W. Koch, *Quantum Theory of the Optical and Electronic Properties of Semiconductors*, 3rd ed. (World Scientific, Singapore, 1994).

[2] T. Yajima and Y. Taira, J. Phys. Soc. Jpn. **47**, 1620 (1979).

[3] N.A. Kurnit, I.D. Abella, and S.R. Hartmann, Phys. Rev. Lett. **13**, 567 (1964).

[4] G. Noll, U. Siegner, S. Shevel, and E.O. Göbel, Phys. Rev. Lett. **64**, 792 (1990).

[5] U. Siegner, D. Weber, E.O. Göbel, D. Bennhardt, V. Heuckeroth, R. Saleh, S.D. Baranovskii, P. Thomas, H. Schwab, C. Klingshirn, J.M. Hvam, and V.G. Lyssenko, Phys. Rev. B **46**, 4564 (1992).

[6] C. Lonsky, P. Thomas, and A. Weller, Phys. Rev. Lett. **63**, 652 (1989).

[7] D. Bennhardt, P. Thomas, A. Weller, M. Lindberg, and S.W. Koch, Phys. Rev. B **43**, 8934 (1991).

[8] V. Heuckeroth, D. Bennhardt, P. Thomas, and H. Vaupel, Int. J. Mod. Phys. B **8**, 935 (1994).

[9] T. Takagahara, Phys. Rev. B **31**, 6552 (1985); **32**, 7013 (1985); J. Lumin. **44**, 347 (1989).

[10] F.R. Shapiro and D. Adler, J. Non-Cryst. Solids **74**, 189 (1985).

[11] M. Grünewald and P. Thomas, Phys. Status Solidi B **94**, 125 (1979); M. Grünewald, P. Thomas, and D. Würtz, *ibid.* **94**, K1 (1979).

[12] N.F. Mott, Philos. Mag. **19**, 835 (1969).

[13] T. Kuhn and F. Rossi, Phys. Rev. B **46**, 7496 (1992).

[14] F. Rossi, P. Poli, and C. Jacoboni, Semicond. Sci. Technol. **7**, 1017 (1992).

[15] A. Stahl and I. Balslev, *Electrodynamics of the Semiconductor Band Edge*, Springer Tracts in Modern Physics Vol. 110 (Springer, Berlin, 1987), and references therein.

[16] H. Böttger and V.V. Bryksin, *Hopping Conduction in Solids* (Akademie-Verlag, Berlin, 1985).

[17] G.D. Mahan, *Many Particle Physics* (Plenum Press, New York, 1981).

[18] U. Dersch, M. Grünewald, H. Overhof, and P. Thomas, J. Phys. C **20**, 121 (1987); M. Grünewald and P. Thomas, J. Non-Cryst. Solids **77&78**, 175 (1985).

[19] H. Müller and P. Thomas, Phys. Rev. Lett. **51**, 702 (1983); J. Phys. C **17**, 5337 (1984).

[20] H. Overhof and P. Thomas, *Electronic Transport in Hydrogenated Amorphous Semiconductors*, Springer Tracts in Modern Physics Vol. 114 (Springer, Berlin, 1989).

[21] A. Miller and E. Abrahams, Phys. Rev. **120**, 745 (1960).

[22] M. Lindberg, R. Binder, and S.W. Koch, Phys. Rev. A **45**, 1865 (1992).

[23] S. Haas, F. Rossi, and T. Kuhn, Phys. Rev. B **53**, 12 855 (1996).

[24] G. Williams, *Molecular Aspects of Multiple Dielectric Relaxation Processes in Solid Polymers*, Advances in Polymer Science (Springer, Berlin, 1979), Vol. 33, p. 59.

[25] S.D. Baranovskii, P. Thomas, and G.J. Adriaenssens, J. Non-Cryst. Solids **190**, 283 (1995).